A Topologically Segregated One-Bead-One-Compound Combinatorial Glycopeptide Library for Identification of Lectin Ligands

Laiqiang Ying,[‡,#] Ruiwu Liu,[§] Jinhua Zhang,[‡] Kit Lam,[§] Carlito B. Lebrilla,[‡,†] and Jacquelyn Gervay-Hague*[,‡]

Department of Chemistry, University of California, Davis, One Shields Ave, Davis, California 95616, Davis Cancer Center, University of California, 4501 X Street, Sacramento, California 95817, and Department of Biochemistry and Molecular Medicine, School of Medicine, University of California, Davis, One Shields Avenue, Davis, California 95616

Received October 15, 2004

A glycopeptide library containing more than 500 000 compounds has been constructed from a combination of Asn-linked carbohydrates using one-bead-one-compound combinatorial methodologies. The library was encoded with peptide markers that were topologically segregated on the interior of the solid support to negate interference with carbohydrate/protein recognition during lectin screening. Both the peptide backbone and carbohydrate components were randomized, but the glycosamine was limited to position 3 at the center of the pentapeptide to evaluate the influence of the peptide backbone in lectin recognition. Of the four lectins that were evaluated, remarkable selectivity was observed with wheat germ agglutinin (WGA), which recognizes *N*-acetyl glucosamine (GlcNAc). From more than 80 000 possible combinations, only six ligands were identified, all possessing GlcNAc. These compounds were independently synthesized, characterized, and evaluated in solution. All six of the glycopeptides showed higher affinity for WGA than GlcNAc, with one having a 4-fold increase. Modeling studies indicate that the peptide backbone is capable of interacting with amino acids in the active site of WGA, but these interactions are not strongly correlated with activity, suggesting that the primary role of the peptide is to properly orient the sugar in the recognition process.

Introduction

Lectins are carbohydrate-specific binding proteins that are found throughout nature. The occurrence of lectins in plants has been known for over a century, yet even today, their biological roles are poorly understood. Plant lectins have served as important tools in the discovery of mammalian lectins and identification of their biological targets. A classical example if this is provided by the characterization of cell surface carbohydrates that define the blood groups.[1]

Lectins engage in multivalent interactions involving several binding sites on the same protein or in systems having several copies of the carbohydrate recognition domain. Crystallographic studies indicate that lectin/carbohydrate interactions tend to occur in rather shallow recognition domains found at the surface of the protein. The carbohydrate typically interacts with the protein through hydrogen bonding, CH$-\pi$ interactions, and metal-mediated processes, but because these are primarily surface interactions, they are relatively weak when only monosaccharides are involved ($K_d \sim 1-10$ mM). Complex carbohydrates exhibit increased lectin affinity ($K_d \sim 1-10$ μM) arising from secondary interactions of the attached carbohydrates with the protein target.

Studies directed toward making large chemical arrays of complex carbohydrates with increased lectin activities have been a major focus of combinatorial chemistry in recent years.[2] However, challenges associated with carbohydrate synthesis, including laborious protecting group manipulations and the need for regio- and stereoselective glycosylations, have prompted others to explore using glycopeptides as mimics of oligosaccharide core structures.[3,4] These glycopeptides contain sugar moieties, which provide specificity of binding by directing the ligand to the oligosaccharide recognition site.[2] The assembly of glycopeptides is considerably more facile than that of oligosaccharides, and the process can be adapted to combinatorial synthesis with either glycosylated amino acid building blocks or by direct glycosylation of the peptide backbone.[5,6]

In recent disclosures, the one-bead-one-compound (OBOC) technology pioneered by Lam et al.[7] was applied to the synthesis of glycopeptide libraries.[8,9] The synthetic history of each glycopeptide was captured on the beads by capping a small percentage of the growing oligomer chain in each synthetic step. In what is termed a ladder synthesis, a series of related fragments was generated on the solid support rather than a single compound.[10] For chemical encoding, the spatial relationship between the coding tag and the testing compound is an important consideration because the coding tag may interfere with screening assays. Ideally, the testing compound should be on the bead's surface and accessible to the screening protein, with the coding tag physically isolated

* Corresponding author. Phone: 530-754-9577. Fax: 530-752-8995. E-mail: gervay@chem.ucdavis.edu.
‡ Department of Chemistry.
§ Davis Cancer Center.
† Department of Biochemistry and Molecular Medicine.
# Current address: Molecular Probes, 29851 Willow Creek Rd., Eugene, OR 97402.

10.1021/cc049836e CCC: $30.25
Published on Web 03/11/2005

Scheme 1. Synthesis of the Encoded Glycopeptide Library

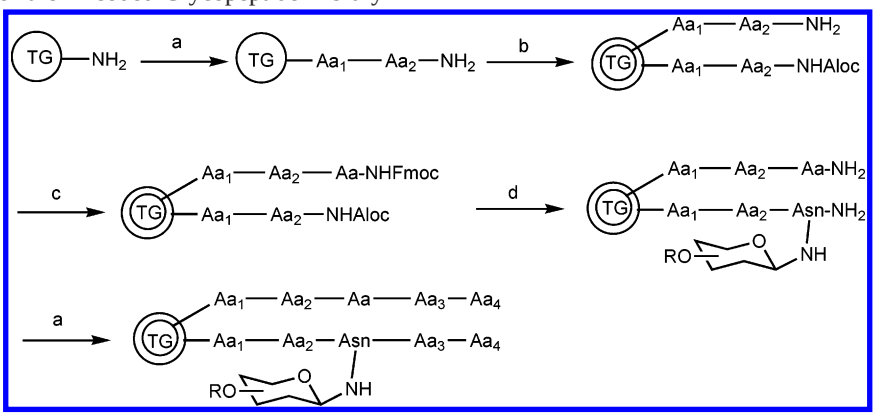

(a) Fmoc-amino acid (Fmoc-Aa) (3 equiv), HOBt (3 equiv), DIC (3 equiv), DMF; 25% piperidine in DMF. Repeat. (b) Aloc-OSu (0.5 equiv), DIEA (2.5 equiv), DCM/ethyl ether. (c) Fmoc-Aa (3 equiv), HOBt (3 equiv), DIC (3 equiv), DMF. (d) $Pd(PPh_3)_4$ (0.25 equiv), $PhSiH_3$ (20 equiv), DCM; Fmoc-Asn-linked sugar (3 equiv), HBTU (3 equiv), HOBt (3 equiv), DIEA (9 equiv), DMF; 25% Piperidine in DMF.

Table 1. Fmoc Asn-Linked Sugar Building Blocks and Natural Amino Acid Tags

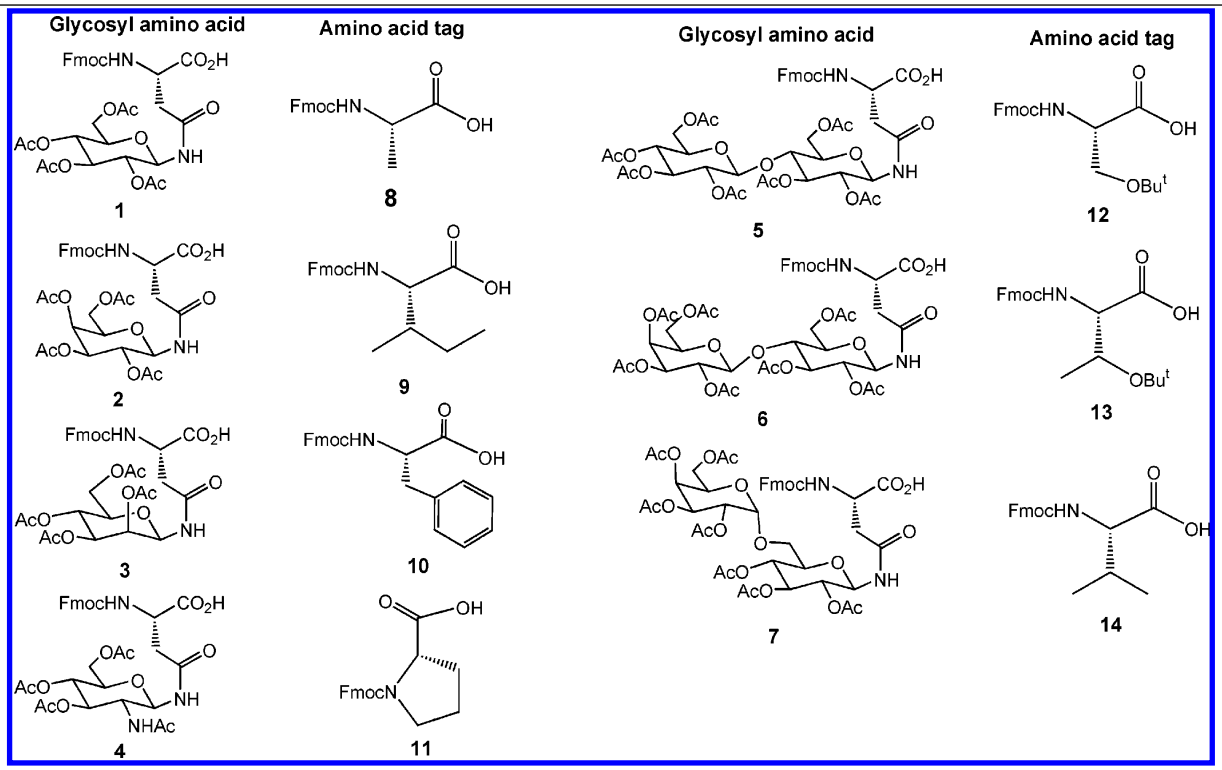

from interactions with the protein. This is feasible in TentaGel resin beads because the interior of the bead is relatively inaccessible to screening probes. Lam and co-workers have previously reported the selective derivatization of solid support surfaces using polyglutamic acid of 30 kDa mw to completely block surface accessible functional groups.[11] They have also reported the use of enzymes such as proteases to topologically modify the bead's surface.[12] Toone nicely applied this so-called bead-shaving methodology in the synthesis of spatially segregated C-glycopeptide libraries.[13] Nevertheless, these technologies are sometimes less than ideal due to difficulties with batch-to-batch reproducibility. To address this shortcoming, a physical approach allowing spatial segregation of the tag and the ligand on a single bead was accomplished by selective protection of the outer bead layer using a biphasic method.[14]

In this report, we apply the biphasic method of topological segregation to the construction of a glycopeptide library derived from 17 different amino acids and 7 different β *N*-linked Asn sugars. Our design features include randomization of the peptide backbone and the carbohydrate content, but we confined the carbohydrate position to the center of a pentapeptide in order to independently evaluate peptide/lectin interactions of active hits. In nature, *N*-glycans are synthesized by glycosylation of a tripeptide beginning with asparagine joined to a variable amino acid (X) with the third residue always serine or threonine. The repertoire of natural glycans is limited by this system. With chemical ligation technologies rapidly evolving, the possibility of breaching the natural sequon (NXS/T) barrier presents itself, and as indicated herein, combinatorial chemistry is an important tool

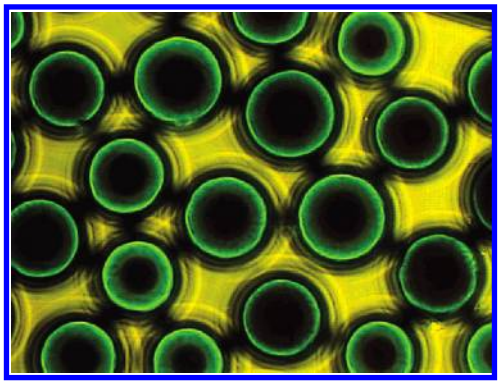

Figure 1. Photomicrograph of topologically segregated bifunctional TentaGel beads. Aloc-protected amine functionalities (green) are present on the surface.

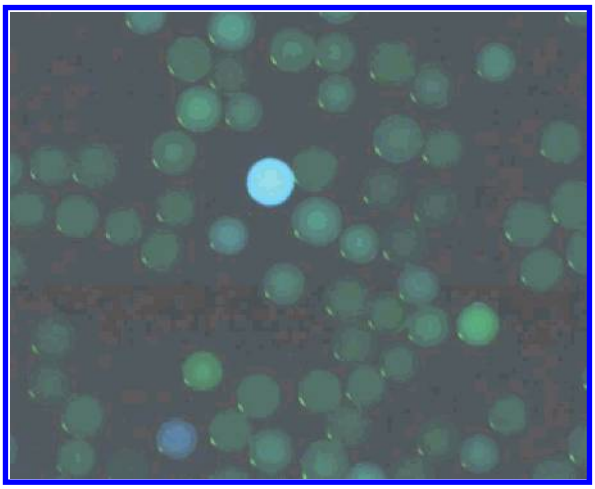

Figure 2. A portion of library beads after incubation with FITC-labeled WGA lectin.

in guiding the design of nonnatural glycopeptides with specific functions.

Results and Discussion

The encoded pentapeptide library was synthesized on TentaGel resin as solid support using the split-and-mix method for the generation of a one-bead-one-compound library (Scheme 1).[7] All the natural amino acids except for Cys, Ile, and Met were included. Seven glycosylated amino acid building blocks, **1**−**7**, were utilized, and each was encoded with a unique naturally occurring amino acid (**8**−**14**), as shown in Table 1. We used natural amino acid tags to code for Asn-linked carbohydrates so that Edman degradation could be used to identify hits. Although others have reported using Edman degradation to characterize glycopeptides, we found this to be tedious and time-consuming owing to marked differences between amino acid and glycosylated amino acid HPLC retention times.

The natural amino acids were incorporated using 9-fluorenylmethoxycarbonyl (Fmoc)/1-hydroxybenzotriazole (HOBt)/1,3-diisopropyl carbodiimide (DIC) methodology, and the glycosylated building blocks were coupled using Fmoc/*O*-benzotriazole-*N*,*N*,*N*′,*N*′-tetramethyluronium hexafluorophosphate (HBTU)/HOBt/diisopropylamine (DIEA) methodology. We chose these coupling conditions on the basis of independent evaluation of coupling efficiency in model studies. The progress of the coupling reactions was monitored using the Kaiser test.[15] After the first two randomized positions were introduced, the beads were selectively protected with an allyloxycarbonyl (Aloc) group in the outer layer (Figure 1) using the biphasic method. Briefly, the resin was swelled in water for 24 h, after which the water was removed by suction, and a solution of AlocOSu and diisopropylethylamine (DIEA) in CH_2Cl_2/diethyl ether were added to the wet beads. Upon completion of the protection step, the resin was split into seven equal portions, and each portion was encoded with the natural amino acid **8**−**14** corresponding to the carbohydrate unit to be introduced in the subsequent transformation. Next, the surface Aloc-protecting group was removed using $Pd(PPh_3)_4$,[16] and each of the Fmoc Asn-linked sugar building blocks **1**−**7** was coupled to the appropriately encoded resin. Subsequently, two more randomized positions were introduced. The carbohydrate acetyl protecting groups were deprotected on-bead using NaOMe/MeOH,[17] and the side-chain protecting groups were removed using reagent K.[18] The resulting 584 647-member library was stored in PBS buffer until it was screened.

Table 2. Lectin Screening Results from the 584 647-Member Glycopeptide Library

lectin	peptide sequence
Bandeiraea simplicifolia BS−I isolectin B4 (α-gal)	no hits
Con A (α-man, α-GLC)	no hits
Lens culinaris (α-man)	YGN(Glc)AF
	YTN(Gal)VY
	PNN(Man)YI
	YFN(Cel)AY
	PYA(Lac)FY
	YYN(GlcNAc)YY
	VYN(Gal)YY
	YAN(Man)WY
	IYN(Cel)YY
	YAN(Lac)YW
	YYN(GlcNAc)WV
wheat germ agglutinin (WGA) (GlcNAc)	SHN(GlcNAc)QG
	FRN(GlcNAc)AS
	RHN(GlcNAc)FA
	RQN(GlcNAc)GN
	VHN(GlcNAc)RQ
	FVN(GlcNAc)SR

Table 3. Mass of Positive Glycopeptides and Peptides[a]

sequence	mass calcd	mass obs
SHN(GlcNAc)QGB **15**	850.331 (MNa^+)	850.367
FRN(GlcNAc)ASB **16**	880.416 (MH^+)	880.447
RHN(GlcNAc)FAB **17**	930.443 (MH^+)	930.504
RQN(GlcNAc)GNB **18**	874.402 (MH^+)	874.421
VHN(GlcNAc)RQB **19**	939.465 (MH^+)	939.524
FVN(GlcNAc)SRB **20**	908.448 (MH^+)	908.469
SHNQGB **21**	647.251 (MNa^+)	647.267
FRNASB **22**	677.337 (MH^+)	677.355
RHNFAB **23**	727.364 (MH^+)	727.392
RQNGNB **24**	671.323 (MH^+)	671.355
VHNRQB **25**	736.385 (MH^+)	736.415
FVNSRB **26**	705.368 (MH^+)	705.401

[a] All MALDI spectra obtained from partially cleaved beads by CNBr.

Library Screening. The biological activity of the glycopeptide library was screened against several lectins. Typi-

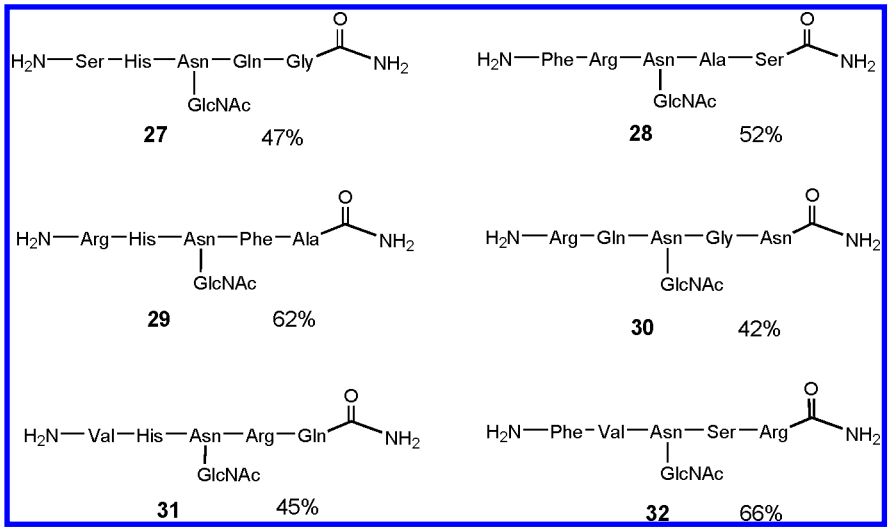

Figure 3. Yields of glycopeptides **27**−**32** synthesized on Rink-amide MBHA resin.

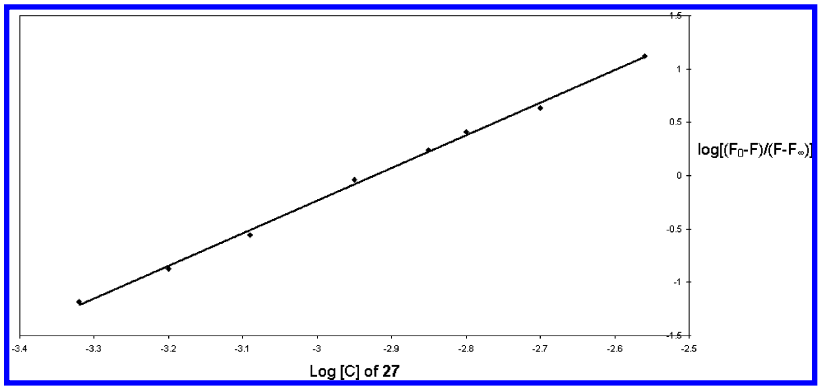

Figure 4. Spectrofluorimetric determination of the association constant (K_a) between WGA and glycopeptide **27**.

Table 4. Association Constants of Saccharides and Glycopeptides with WGA

compd	K_a, $\times 10^3$ M^{-1}
GlcNAc	0.4
GlcNAc-β-(1 → 4)GlcNAc	4.2
27	0.84
28	1.34
29	1.11
30	1.25
31	1.01
32	1.54

cally, a portion of the library (∼250 000 beads) was incubated with FITC-labeled lectins. The brightest fluorescent beads were selected for decoding with the assistance of a fluorescence microscope (Figure 2). From the results obtained from automated protein sequencing (Table 2), the glycopeptide library did not bind to *Bandeiraea simplicifolia* BS-I isolectin B4, which is selective for α-galactose. Recall that this library contains galactose β-linked to asparagine (Asn). There were also no positive hits for concanavalin A, which is an α-mannose-, α-glucose-binding lectin, indicating that the peptide component is not able to compensate for specificity of the glycosidic linkage in these lectins. In contrast, 11 positive hits, all containing tyrosine residues, were found to bind *Lens culinaris*, which is an α-man binding lectin. This lectin showed no selectivity for the sugars, suggesting that the peptides may be providing the primary interactions with the lectin. Most interestingly, six glycopeptides containing only GlcNAc were detected as positive hits to wheat germ agglutinin (WGA) lectin, which is a GlcNAc-specific binding lectin. This would suggest that WGA recognition depends on both the carbohydrate and the peptide backbone, because there are over 80 000 possible combinations of glycopeptides containing GlcNAc, and only 6 high-affinity ligands were identified.

Validation of Positive Hits. To verify the results from the WGA screening, we independently synthesized the positive glycopeptides along with the corresponding peptide backbones, in which the GlcNAc−Asn was replaced with Asn. To enable cyanogen bromide (CNBr) cleavage from the resin for MS characterization, the TentaGel resin was first coupled with 10% methionine, then the glycopeptides (**15**−**20**) and peptides (**21**−**26**) were synthesized in parallel. A portion of beads from each of the glycopeptide and peptide samples was treated with CNBr, and the products were analyzed by MALDI-MS. The reported masses in Table 3, which were obtained with external calibration, confirm the identity of the compounds. All of the bead-bound glycopeptides showed strong fluorescence when incubated with FITC−WGA, whereas the peptides on solid support showed only background fluorescence. These studies indicated that GlcNAc was required for WGA recognition, but the contribution of the peptide backbone could not be independently evaluated on solid support.

Fluorescence Measurements of Glycopeptide/WGA Interactions. We next turned to solution-phase binding

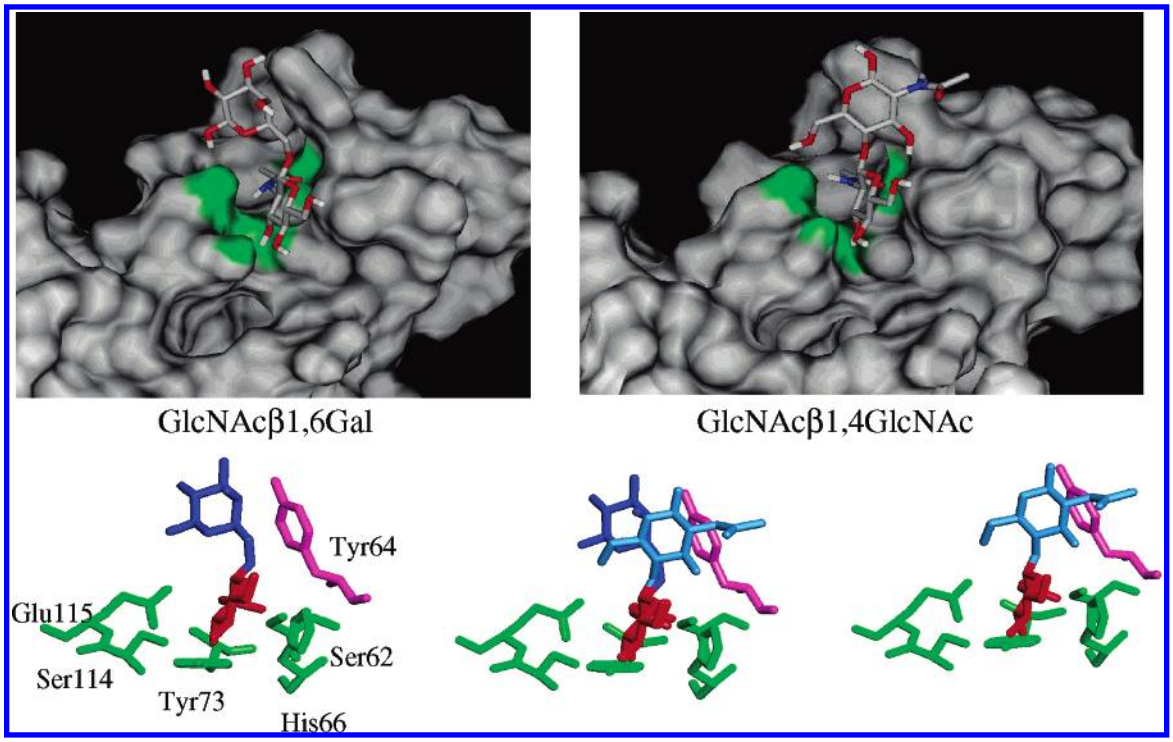

Figure 5. (Above) The crystal structures of WGA complexed with GlcNAc-β-(1 → 6)Gal (left) and GlcNAc-β-(1 → 4)GlcNAc (right). (Below) Representation of carbohydrate/protein interactions. The green residues are protein amino acids as labeled. The red structure is GlcNAc, and the dark blue structure is Gal (left), whereas the cornflower blue structure on the right is the reducing end GlcNAc. The central picture is an overlay of the two structures. Tyr 64 (pink) is involved in secondary interactions with both of the reducing end sugars.

Table 5. Primary Interactions (<3.2 Å) between GlcNAc (red) and WGA, Determined Using MacroModel 7.0

peptide			protein residue	distance (Å)
GlcNAc	C-2 NH	HBD	Glu115 OE2	1.8
	C-2 NH	HBD	Glu115 OE1	3.1
	C-4 OH	HBA	Ser114 HG	1.9
	C-3 OH	HBD	Tyr73 OH	1.8
	C-2 CO	HBA	His66 HD1	2.2
	C-2 CO	HBA	Ser62 HG	1.7
	C-2 H	CH−π	His66	2.3
	C-4 H	CH−π	His66	3.1
	C-2 CH_3	CH−π	Tyr73	3.0

affinity studies to alleviate complications from polyvalent interactions provided by the solid support and to assess the relative contributions of the peptide backbones. To test the binding affinity of each glycopeptide in solution, the six glycopeptides (**27**−**32**) were synthesized on Rink-amide MBHA resin and cleaved by treatment with TFA. All of the glycopeptides were purified on semipreparative RP-HPLC; the yields of purified glycopeptides were between 42 and 66% (Figure 3).

The binding of GlcNAc-containing ligands to WGA has been widely studied using equilibrium dialysis,[19] fluorescence,[20,21] NMR,[22] X-ray diffraction techniques,[23] isothermal titration calorimetry, and enzyme-linked lectin-binding assays.[23−25] We and others have found the fluorescence method first developed by Nathan Sharon to be well-suited for the task.[27,28] In 1973, Sharon found that WGA presents a typical tryptophan fluorescence spectrum at 348 nm.[20,29] Upon addition of GlcNAc analogues, a blue shift of the fluorescence spectrum and an increase of fluorescence intensity are observed. When we applied this method to the evaluation of WGA/glycopeptide interactions, we also observed fluorescence quenching. By measuring the change in fluorescence intensity of WGA upon the addition of different concentrations of glycopeptides, we determined the association constants (K_a). WGA showed the maximum fluorescence intensity at a wavelength of 348 nm with an excitation wavelength at 280 nm. Upon addition of the glycopeptide, the fluorescence intensity continually decreased until WGA was saturated with ligand. To determine the association constant, the relative fluorescence intensity of WGA saturated with ligand, F_∞, was obtained by extrapolating a plot of $1/(F_0 - F)$ versus 1/[C] to 0; where F_0 is the fluorescence of WGA alone, F is the fluorescence of WGA/glycopeptide mixtures, and C is the concentration of glycopeptide. The value of F_∞ was incorporated into a plot of log $[(F_0 - F)/(F - F_\infty)]$ vs log[C]. The value of $-\log K_a$ for the complex equals the value of log[C] at log $[(F_0 - F)/(F - F_\infty)] = 0$ (Figure 4). In this manner, the association constants for the six glycopeptides and two saccharides (GlcNAc and GlcNAcβ(1 → 4)GlcNAc) were measured (Table 4). As shown in Figure 4, GlcNAcβ(1 → 4)GlcNAc showed more than 10 times higher WGA affinity than GlcNAc, which is consistent with the findings of others.[30] However, it is evident that incorporation into an appropriate peptide backbone significantly enhances GlcNAc activity, because all of the glycopeptides **27**−**32** showed higher affinity relative to the monosaccharide, especially glycopeptide **32** (almost four times higher than GlcNAc).

Molecular Dynamics Modeling for Glycopeptide Binding to WGA. To better understand WGA/ligand interactions, the six glycopeptides **27**−**32** were docked into the crystal structure of WGA.[25] Molecular dynamics calculations were performed using simulated annealing in MacroModel 7.0.

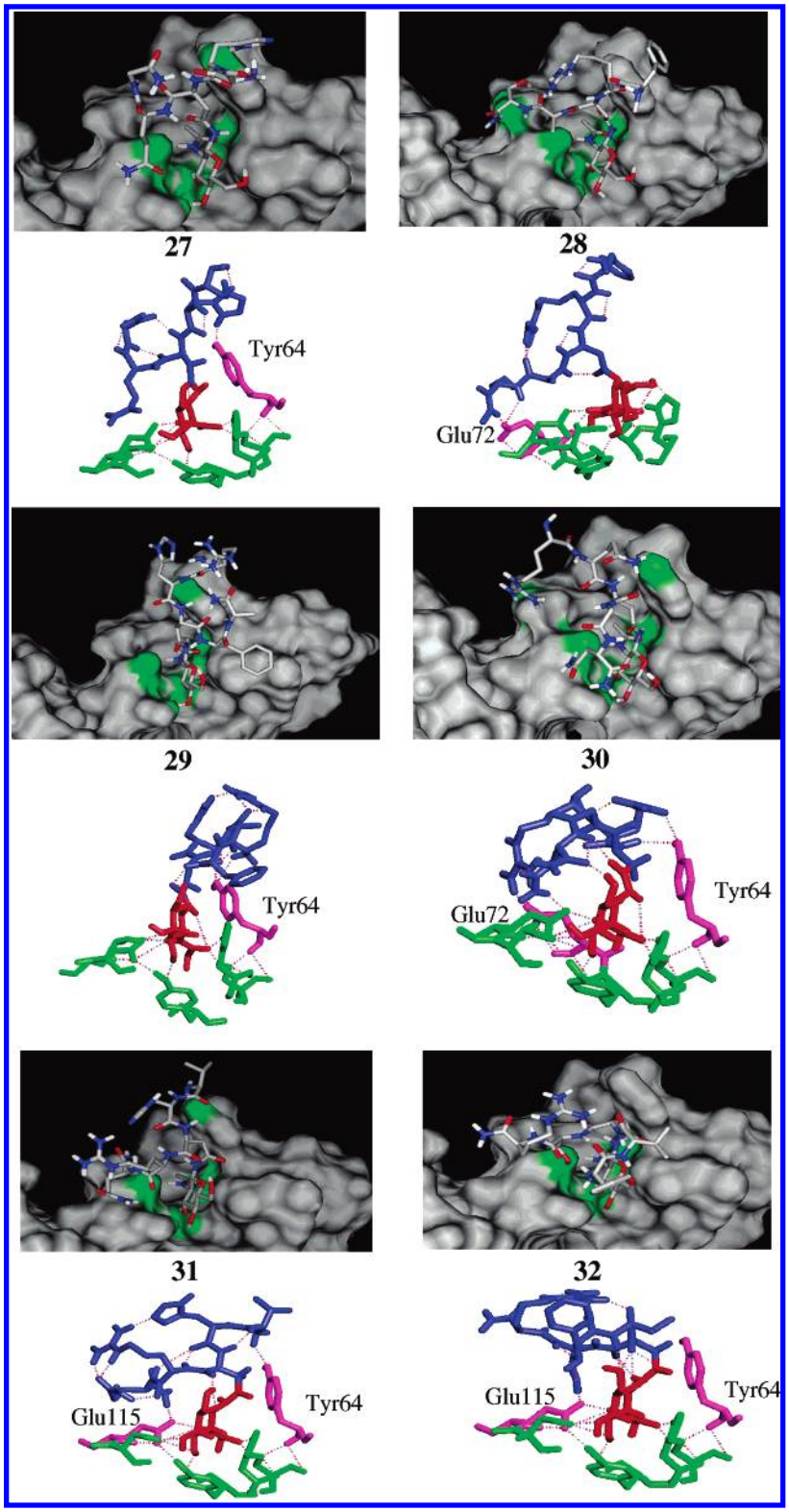

Figure 6. Models of WGA/glycopeptide complexes.

The crystal structure of the protein was maintained, and the GlcNAc from the glycopeptide was properly aligned in the binding site. As shown in the crystal structure (Figure 5), GlcNAcβ(1 → 6)Gal and GlcNAcβ(1 → 4)GlcNAc have similar WGA binding modes. In each case, the nonreducing end GlcNAc adopts the same conformation to form hydrogen bonds with Ser 62, His 66, Tyr 73, Ser 114, and Glu 115, and the Gal or the reducing end GlcNAc forms CH$-\pi$ interactions with Tyr 64 (Table 5).

Since the GlcNAc adopts the same binding mode in both crystal structures, we fixed the conformation of GlcNAc in each of the glycopeptides and investigated the interactions of the peptide backbone with WGA lectin. As shown in Figure 6, in addition to the primary interactions between GlcNAc and WGA (Table 5), the peptides participate in secondary interactions with WGA (Table 6). With the exception of **28**, all of the glycopeptides show secondary interactions with Tyr 64. These involve not only CH$-\pi$

Table 6. Secondary Interactions (<3.2 Å) between Peptides and WGA Determined Using MacroModel

peptide				protein residue	distance (Å)
peptide **27**	His	NH	HBD	Tyr64 OH	1.9
	Asn	CH_2	CH-π	Tyr64	2.6
peptide **28**	Ser	NH	HBD	Glu72 OE2	3.0
	NME	NH	HBD	Glu72 OE2	1.7
peptide **29**	His	NH	HBD	Tyr64 OH	1.9
	Arg	NH	HBD	Tyr64 OH	3.0
	Asn	CH_2	CH$-\pi$	Tyr64	2.5
peptide **30**	Gln	NH	HBD	Tyr64 OH	2.3
	Asn	NH	HBD	Tyr64 OH	2.5
	Asn	NH	HBD	Glu115 OE2	2.1
	Arg	NH	HBD	Glu72 OE2	1.7
	Arg	NH	HBD	Glu72 OE1	2.7
	Asn	CH_2	CH$-\pi$	Tyr64	2.5
peptide **31**	Val	NH	HBD	Tyr64 OH	2.1
	NME	NH	HBD	Glu115 OE2	1.7
	Asn	CH_2	CH$-\pi$	Tyr64	3.1
peptide **32**	Ser	OH	HBD	Glu115 OE2	1.7
	Asn	CH_2	CH$-\pi$	Tyr64	2.7

interactions, as is observed in the disaccharides, but also NH hydrogen bond donation (HBD). HBD is also seen with Glu 72 and Glu 115. If secondary interactions were the dominant factor contributing to the enhanced binding affinities relative to GlcNAc, we would expect the peptide having the most interactions (**30**) to have the highest affinity. But in fact, **32**, which only has two secondary interactions with WGA, has the highest affinity. These results suggest that the primary role of the peptide is to serve as a scaffold that preferentially orients the carbohydrate in a favorable geometry for recognition.

Conclusions

A novel peptide encoding method has been applied to the construction of glycopeptide libraries as ligands for carbohydrate-binding proteins. Topologically segregated beads consisting of a surface ligand and core-coding molecule minimize nonspecific receptor interactions and the methodology enables straightforward and unambiguous decoding with an automatic microsequencer. A large library of pentapeptides with randomized peptide and carbohydrate components was screened against four different lectins, and while two of the lectins showed no affinity for any members of the library, several hits were identified for *Lens culinaris* and wheat germ agglutinin. *Lens culinaris* selected out glycopeptides having a high content of tyrosine, suggesting that protein/protein interactions were at play. In contrast, six hits were identified from the WGA screen, all having GlcNAc sugars. These compounds were prepared independently for solution-phase binding studies, which indicated that the glycopeptides have higher affinity than the monosaccharide. Molecular dynamics studies showed that the peptide backbone was able to engage in secondary interactions, some similar to those observed in the crystal structures of GlcNAc-β-(1 → 6)Gal and GlcNAc-β-(1 → 4)GlcNAc. However, glycopeptide binding affinity did not correlate with increased secondary interactions, suggesting that the peptides' primary role is as a scaffold for ligand display.

Experimental Section

Materials and General Methods. All chemicals were used as supplied without further purification. Solvents (MeOH 99.8%, CH_2Cl_2 99.8%, DMF 99.8%) were purchased in anhydrous Sure/Seal bottles from Aldrich, used without further purification, and stored under argon. Allyloxycarbonyl *N*-hydroxysuccinimide ester (AlocOSu) was purchased from Senn Chemicals. Fmoc-protected amino acids were purchase from Advanced ChemTech and Novabiochem. TentaGel S NH_2 resin was purchased from Rapp Polymere Gmbh (Tubingen, Germany). FITC-labeled lectins were purchased from Sigma (3 mol FITC per mol of lectin). Column chromatography was conducted using flash silica gel (32−63 μm) available from Scientific Adsorbents and solvents purchased from EM Science. Solid-phase peptide coupling reactions were monitored using the Kaiser test, and solution-phase reactions were monitored by TLC performed on silica gel 60 F_{254} aluminum-backed sheets with detection by UV radiation or charring in a cerium molybdate solution. NMR experiments (1D and 2D) were conducted on Inova 400 MHz or Bruker DRX500 MHz spectrometers at 298 K. RP-HPLC preparative separations were carried out on a Vydac C18 column (10 × 250 mm). Solvents: (A) H_2O and (B) CH_3-CN with UV detection at 220 and 254 nm. Peptide sequence was determined by Perkin-Elmer/Applied Biosystems protein sequencer (ABI Procise 494). Mass spectra were recorded in MALDI-FTMS instrument (IonSpec Corp., Irvine, CA).

General Procedure for Synthesis of Glycosylated Asparagine Derivatives. (1) Method A. To a solution of Fmoc-Asp-O^{t}Bu (0.5 mmol) and per-*O*-acetyl glycosyl azide (0.5 mmol) in dry CH_2Cl_2 was added triethylphosphine (0.5 mmol) under argon at −30 °C. The solution was slowly warmed to room temperature and stirred overnight. The solution was concentrated in vacuo and extracted with EtOAc. The extracts were washed with 5% citric acid, water, and brine; dried (anhyd Na_2SO_4); and concentrated. The residue was purified by column chromatography (silica gel, ethyl acetate/hexane = 3:1).

(2) Method B. To a solution of per-*O*-acetyl glycosyl azide (200 mg) in 20 mL of dry methanol was added 20 mg 10% Pd/C (for mannose, 40 mg of Raney nickel was added), and the solution was bubbled with H_2 ~3 to 4 h at 0 °C. TLC showed the reaction was completed. The Pd/C was filtered, and the solution was concentrated to dryness. To a solution of Fmoc-Asp-O^{t}Bu (0.5 mmol) in dry CH_2Cl_2 was added HOBt (0.5 mmol) and PS-carbodiimide (1.0 mmol). The solution was stirred under argon at 0 °C for 15 min. The per-*O*-acetyl glycopyranosylamine (0.5 mmol) was added to the mixture and stirred overnight. The resin was filtered and washed with CH_2Cl_2. The filtrate was washed with 10% $NaHCO_3$, water, and brine; dried (anhyd Na_2SO_4); and evaporated. The residue was purified by column chromatography (silica gel, ethyl acetate/hexane = 3:1).

General Method for Cleavage of α-*tert*-Butyl Ester Group. A 0.5 mmol portion of Fmoc-Asn(sugar)-*O*-Bu^t was dissolved in 6 mL of 50% TFA in CH_2Cl_2. After 30 min, the solution was removed, and the product was triturated with ether to give a white powder. The crude was >95%

pure and used directly for solid-phase synthesis of glycopeptide libraries.

***N*$^{\alpha}$-(9-Fluorenylmethyloxycarbonyl)-*N*$^{\omega}$-(2,3,4,6-tetra-*O*-acetyl-β-D-glucopyranosyl)-L-asparagine (1).** The *tert*-butyl ester of **1** was prepared from per-*O*-acetyl glucosyl azide[31] in 46% yield using method A and 54% using method B. $[\alpha]^{25}_{D}$ +31.3° (*c* 0.5, $CHCl_3$). ^{1}H NMR ($CDCl_3$, 500 MHz) δ 1.45 (s, 9H, *t*-Bu), 2.03, 2.04, 2.05, 2.07 (4s, 12H, 4 × OAc), 2.68−2.89 (m, 2H, Asn-β-CH_2), 3.79 (m, 1H, H-5), 4.04 (d, J = 11.6 Hz, 1H, H-6), 4.20 (t, J = 7.0 Hz, 1H, Fmoc-CH), 4.26−4.42 (m, 3H, H-6′, Fmoc-CH_2), 4.47 (m, 1H, Asn-α-CH), 4.92 (t, J = 9.6 Hz, 1H, H-2), 5.06 (t, J = 9.6 Hz, 1H, H-4), 5.24 (t, J = 9.2 Hz, 1H, H-1), 5.31 (t, J = 9.6 Hz, 1H, H-3), 5.93 (d, J = 8.0 Hz, 1H, Asn-α-NH), 6.42 (d, J = 8.8 Hz, 1H, 1-NH), 7.31(app-t, 2H, Fmoc-Ar), 7.40 (app-t, 2H, Fmoc-Ar), 7.60 (d, J = 7.3 Hz, 2H, Fmoc-Ar), 7.76 (d, J = 7.3 Hz, 2H, Fmoc-Ar). ^{13}C NMR ($CDCl_3$, 100 MHz) δ 20.7, 20.8, 20.8, 28.0, 38.2, 47.2, 51.1, 61.2 (C-6), 67.3, 68.1 (C-4), 70.7 (C-2), 72.7 (C-5), 73.8 (C-3), 78.3 (C-1), 82.6, 120.1, 125.3, 127.2, 127.9, 141.4, 143.9, 144.0, 156.3, 169.7, 169.9, 170.0, 170.7, 170.9, 171.3. FAB-HRMS calcd for $C_{37}H_{44}N_2O_{14}Na$ $[M + Na]^+$: 763.2678. Found: 763.2648.

Compound **1** was obtained in quantitative yield from hydrolysis of the *tert*-butyl ester. $[\alpha]^{25}_{D}$ +34.9° (*c* 0.8, $CHCl_3$). ^{1}H NMR ($CDCl_3$, 500 MHz) δ 2.03, 2.04, 2.06 (3s, 12H, 4 × OAc), 2.75−2.94 (m, 2H, Asn-β-CH_2), 3.83 (m, 1H, H-5), 4.08 (d, J = 12.0 Hz, 1H, H-6), 4.22 (t, J = 7.0 Hz, 1H, Fmoc-CH), 4.30 (dd, J = 12.0 Hz, 4.0 Hz, 1H, H-6′), 4.35−4.44 (m, 2H, Fmoc-CH_2), 4.61 (m, 1H, Asn-α-CH), 4.94 (t, J = 9.6 Hz, 1H, H-2), 5.08 (t, J = 9.6 Hz, 1H, H-4), 5.27 (t, J = 9.2 Hz, 1H, H-1), 5.34 (t, J = 9.6 Hz, 1H, H-3), 6.17 (d, J = 8.0 Hz, 1H, Asn-α-NH), 6.75 (d, J = 8.8 Hz, 1H, 1-NH), 7.31(app-t, 2H, Fmoc-Ar), 7.40 (app-t, 2H, Fmoc-Ar), 7.59 (d, J = 7.3 Hz, 2H, Fmoc-Ar), 7.76 (d, J = 7.3 Hz, 2H, Fmoc-Ar). ^{13}C NMR ($CDCl_3$, 125 MHz) δ 20.8, 20.9, 37.8, 47.2, 50.5, 61.8 (C-6), 67.8, 68.2 (C-4), 70.8 (C-2), 72.7 (C-5), 73.9 (C-3), 78.3 (C-1), 120.2, 125.3, 127.3, 128.0, 141.5, 143.7, 143.8, 156.6, 169.8, 169.9, 170.2, 171.0, 171.5, 171.7, FAB-HRMS calcd for $C_{33}H_{36}N_2O_{14}$: 684.2167. Found: 707.2043 [M + Na].

***N*$^{\alpha}$-(9-Fluorenylmethyloxycarbonyl)-*N*$^{\omega}$-(2,3,4,6-tetra-*O*-acetyl-β-D-galactopyranosyl)-L-asparagine (2).** The *tert*-butyl ester of **2** was prepared from per-*O*-acetyl galactosyl azide[31] in 40% yield using method A and 52% using method B. $[\alpha]^{25}_{D}$ +32.2° (*c* 0.5, $CHCl_3$). ^{1}H NMR ($CDCl_3$, 500 MHz) δ 1.45 (s, 9H, *t*-Bu), 1.99, 2.02, 2.04, 2.08 (4s, 12H, 4 × OAc), 2.65−2.89 (m, 2H, Asn-β-CH_2), 4.00−4.12 (m, 3H, H-5, H-6, H-6′), 4.22 (t, J = 7.0 Hz, 1H, Fmoc-CH), 4.30−4.44 (m, 2H, Fmoc-CH_2), 4.51 (m, 1H, Asn-α-CH), 5.08−5.16 (m. 2H, H-2, H-3), 5.20 (t, J = 8.8 Hz, 1H, H-1), 5.41 (dd, J = 2.4 Hz, 0.6 Hz, 1H, H-4), 5.93 (d, J = 8.8 Hz, 1H, Asn-α-NH), 6.42 (d, J = 8.8 Hz, 1H, 1-NH), 7.30 (app-t, 2H, Fmoc-Ar), 7.40 (app-t, 2H, Fmoc-Ar), 7.60 (d, J = 7.4 Hz, 2H, Fmoc-Ar), 7.76 (d, J = 7.4 Hz, 2H, Fmoc-Ar). ^{13}C NMR ($CDCl_3$, 100 MHz) δ 20.7, 20.7, 20.8, 20.9, 28.0, 38.1, 47.2, 51.1, 61.2 (C-6), 67.2 (C-4), 67.3, 68.4 (C-2), 70.8 (C-3), 72.5 (C-5), 78.5 (C-1), 82.6, 120.1, 125.3, 127.2, 127.8, 141.4, 143.9, 144.0, 156.3, 169.9, 170.1, 170.5, 170.8, 171.6. FAB-HRMS calcd for $C_{37}H_{44}N_2O_{14}Na$ $[M + Na]^+$: 763.2678. Found: 763.2668.

Compound **2** was obtained in quantitative yield from hydrolysis of the *tert*-butyl ester. $[\alpha]^{25}_{D}$ +46.0° (*c* 0.5, $CHCl_3$). ^{1}H NMR ($CDCl_3$, 500 MHz) δ 2.01, 2.05, 2.16 (3s, 12H, 4 × OAc), 2.79−2.97 (m, 2H, Asn-β-CH_2), 4.12−4.16 (m, 3H, H-5, H-6, H-6′), 4.22 (t, J = 7.0 Hz, 1H, Fmoc-CH), 4.39 (m, 2H, Fmoc-CH_2), 4.61 (m, 1H, Asn-α-CH), 5.11−5.15 (m. 2H, H-2, H-3), 5.32 (t, J = 8.8 Hz, 1H, H-1), 5.50 (broad s, 1H, H-4), 6.29 (d, J = 8.8 Hz, 1H, Asn-α-NH), 6.56 (d, J = 8.8 Hz, 1H, 1-NH), 7.31 (app-t, 2H, Fmoc-Ar), 7.40 (app-t, 2H, Fmoc-Ar), 7.60 (d, J = 7.4 Hz, 2H, Fmoc-Ar), 7.76 (d, J = 7.4 Hz, 2H, Fmoc-Ar). ^{13}C NMR ($CDCl_3$, 125 MHz) δ 20.7, 20.8, 20.9, 37.9, 47.2, 50.3, 61.3 (C-6), 67.4 (C-4), 67.7, 68.8 (C-2), 71.0 (C-3), 72.3 (C-5), 78.5 (C-1), 120.2, 125.4, 127.3, 128.0, 141.5, 143.8, 143.9, 156.6, 170.3, 170.5, 171.0, 171.3, 173.0. FAB-HRMS calcd for $C_{33}H_{36}N_2O_{14}$: 684.2167. Found: 707.2059 [M + Na].

***N*$^{\alpha}$-(9-Fluorenylmethyloxycarbonyl)-*N*$^{\omega}$-(2,3,4,6-tetra-*O*-acetyl-β-D-mannopyranosyl)-L-asparagine (3).** The *tert*-butyl ester of **3** was prepared from per-*O*-acetyl mannosyl azide[31] in 46% yield using method A and 42% using method B. $[\alpha]^{25}_{D}$ +9.7° (*c* 0.3, $CHCl_3$). ^{1}H NMR ($CDCl_3$, 500 MHz) δ 1.45 (s, 9H, *t*-Bu), 2.03, 2.06, 2.07, 2.08 (4s, 12H, 4 × OAc), 2.75−2.94 (m, 2H, Asn-β-CH_2), 3.75 (m, 1H, H-5), 4.03 (d, J = 12.5 Hz, 1H, H-6), 4.22 (t, J = 7.5 Hz, 1H, Fmoc-CH), 4.27−4.35 (m, 2H, H-6′, Fmoc-CH_2), 4.37−4.48 (m, 2H, Fmoc-CH_2, Asn-α-CH), 5.10 (dd, J = 10.0 Hz, 3.5 Hz, 1H, H-3), 5.23 (t, J = 10.0 Hz, 1H, H-4), 5.38 (d, J = 3.5 Hz, 1H, H-2), 5.55 (d, J = 9.0 Hz, 1H, H-1), 5.92 (d, J = 9.0 Hz, 1H, Asn-α-NH), 6.65 (d, J = 9.0 Hz, 1H, 1-NH), 7.32 (app-t, 2H, Fmoc-Ar), 7.40 (app-t, 2H, Fmoc-Ar), 7.60 (d, J = 7.4 Hz, 2H, Fmoc-Ar), 7.75 (d, J = 7.4 Hz, 2H, Fmoc-Ar). ^{13}C NMR ($CDCl_3$, 125 MHz) δ 20.7, 20.8, 20.9, 21.0, 28.0, 38.6, 47.2, 51.2, 62.2 (C-6), 65.2 (C-4), 67.4, 70.0 (C-2), 71.7 (C-3), 74.3 (C-5), 76.1 (C-1), 83.0, 120.1, 125.3, 127.2, 127.9, 141.4, 143.9, 143.9, 156.4, 169.8, 169.8, 170.0, 170.5, 170.8. FAB-HRMS calcd for $C_{37}H_{44}N_2O_{14}Na$ $[M + Na]^+$: 763.2678. Found: 763.2649.

Compound **3** was obtained in quantitative yield from hydrolysis of the *tert*-butyl ester. $[\alpha]^{25}_{D}$ +18.1° (*c* 0.6, $CHCl_3$). ^{1}H NMR ($CDCl_3$, 500 MHz) δ 1.98, 2.05, 2.07, 2.22 (4s, 12H, 4 × OAc), 2.76−2.97 (m, 2H, Asn-β-CH_2), 3.79 (m, 1H, H-5), 4.09 (d, J = 12.5 Hz, 1H, H-6), 4.22 (t, J = 7.5 Hz, 1H, Fmoc-CH), 4.29 (dd, J = 12.5 Hz, 5.0 Hz, 1H, H-6′), 4.38 (m, 2H, Fmoc-CH_2), 4.60 (m, 1H, Asn-α-CH) 5.14 (dd, J = 10.0 Hz, 3.5 Hz, 1H, H-3), 5.24 (t, J = 10.0 Hz, 1H, H-4), 5.39 (broad s, 1H, H-2), 5.55 (d, J = 9.0 Hz, 1H, H-1), 6.13 (d, J = 9.0 Hz, 1H, Asn-α-NH), 6.72 (d, J = 9.0 Hz, 1H, 1-NH), 7.31 (app-t, 2H, Fmoc-Ar), 7.40 (app-t, 2H, Fmoc-Ar), 7.58 (d, J = 7.4 Hz, 2H, Fmoc-Ar), 7.76 (d, J = 7.4 Hz, 2H, Fmoc-Ar). ^{13}C NMR ($CDCl_3$, 125 MHz) δ 20.7, 20.9, 21.0, 21.1, 38.0, 47.2, 50.5, 62.3 (C-6), 65.3 (C-4), 67.7, 69.9 (C-2), 71.7 (C-3), 74.4 (C-5), 76.4 (C-1), 120.2, 125.3, 127.3, 128.0, 141.5, 143.8, 143.9, 156.5, 169.9, 170.3, 170.8, 171.0, 172.9. FAB-HRMS calcd for $C_{33}H_{36}N_2O_{14}$: 684.2167. Found: 707.2045 [M + Na].

***N*$^{\alpha}$-(9-Fluorenylmethyloxycarbonyl)-*N*$^{\omega}$-(2-acetamido-3,4,6-tetra-*O*-acetyl-2-deoxy-β-D-glucopyranosyl)-L-aspar-**

agine (4). Compound **4** was obtained in quantitative yield from hydrolysis of the *tert*-butyl ester.[32] $[\alpha]^{25}_D$ +3.5° (*c* 0.5, DMSO). ^{1}H NMR (DMSO, 500 MHz) δ 1.72 (s, 3H, NAc), 1.90, 1.96, 1.99 (3s, 9H, 3 OAc), 2.46−2.67 (m, 2H, Asn-β-CH_2), 3.81 (m, 1H, H-5), 3.87 (m, 1H, H-2), 3.94 (d, J = 12.0 Hz, 1H, H-6), 4.16−4.29 (m, 4H, H-6′, Fmoc-CH, Fmoc-CH_2), 4.38 (m, 1H, Asn-α-CH), 4.82 (t, J = 9.5 Hz, 1H, H-3), 5.09 (t, J = 9.5 Hz, 1H, H-4), 5.17 (t, J = 9.5 Hz, 1H, H-1), 7.32 (app-t, 2H, Fmoc-Ar), 7.42 (app-t, 2H, Fmoc-Ar), 7.51 (d, J = 8.5 Hz, 1H, Asn-α-NH), 7.71 (d, J = 7.3 Hz, 2H, Fmoc-Ar), 7.89 (d, J = 7.3 Hz, 2H, Fmoc-Ar), 8.58 (d, J = 9.0 Hz, 1H, 1-NH). ^{13}C NMR (DMSO, 125 MHz) δ 20.8, 20.9, 36.8, 46.6, 50.0, 52.1 (C-2), 61.8 (C-6), 65.7, 68.3 (C-3), 72.3 (C-5), 73.4 (C-4), 78.1 (C-1), 120.1, 125.3, 127.1, 127.7, 140.7, 143.8, 156.9, 169.3, 169.5, 169.8, 170.1, 173.0. HRMS calcd for $C_{33}H_{37}N_2O_{13}$: 683.2326. Found: 706.2206 [M + Na].

***N*$^\alpha$-(9-Fluorenylmethyloxycarbonyl)-*N*$^\omega$-[2,3,6-tri-*O*-acetyl-4-*O*-(2,3,4,6-tetra-*O*-acetyl-*β*-D-glucopyranosyl)-*β*-D-glucopyranosyl]-L-asparagine (5).** The *tert*-butyl ester of **5** was prepared from per-*O*-acetyl cellobiosyl azide[31] in 22% yield using method A and 35% using method B. $[\alpha]^{25}_D$ +2.8° (*c* 0.7, $CHCl_3$). ^{1}H NMR (CDCl3, 500 MHz) δ 1.45 (s, 9H, *t*-Bu), 1.98, 2.02, 2.04, 2.05, 2.06, 2.08, 2.09 (7s, 21H, 7 × OAc), 2.67−2.85 (m, 2H, Asn-β-CH_2), 3.63−3.76 (m, 3H, H-5′ H-5, H-4), 4.04 (dd, J = 2.5 Hz, 12.5 Hz, 1H, H-6″), 4.15 (m, 1H, H-6), 4.22 (t, J = 7.0 Hz, 1H, Fmoc-CH), 4.29−4.54 (m, 6H, Fmoc-CH_2, Asn-α-CH, H-1′, H-6′, H-6‴), 4.85 (t, J = 9.5 Hz, 1H, H-2), 4.92 (t, J = 9.5 Hz, 1H, H-2′), 5.07 (t, J = 9.5 Hz, 1H, H-4′), 5.14 (t, J = 9.5 Hz, 1H, H-3′), 5.18 (t, J = 9.5 Hz, 1H, H-1), 5.30 (t, J = 9.5 Hz, 1H, H-3), 5.94 (d, J = 8.5 Hz, 1H, Asn-α-NH), 6.39 (d, J = 9 Hz, 1H, 1-NH), 7.31 (app-t, 2H, Fmoc-Ar), 7.40 (app-t, 2H, Fmoc-Ar), 7.60 (d, J = 7.5 Hz, 2H, Fmoc-Ar), 7.75 (d, J = 7.5 Hz, 2H, Fmoc-Ar). ^{13}C NMR ($CDCl_3$, 100 MHz) δ 20.7, 20.8, 21.0, 28.0, 38.2, 47.2, 51.1, 61.7 (C-6′), 61.9 (C-6), 67.3 (C-4′), 67.9, 70.9 (C-2′), 71.6 (C-5′), 72.1 (C-3′), 72.2 (C-2), 73.0 (C-3), 74.7 (C-5), 76.3 (C-4), 78.2 (C-1), 82.6, 100.8 (C-1′), 120.1, 125.3, 127.2, 127.9, 141.4, 143.9, 144.0, 156.3, 169.1, 169.4, 169.5, 169.9, 170.3, 170.6, 170.7, 171.5. FAB-HRMS calcd for $C_{49}H_{60}N_2O_{22}Na$ [M + Na]$^+$: 1051.3518. Found: 1051.3585.

Compound **5** was obtained in quantitative yield from hydrolysis of the *tert*-butyl ester. $[\alpha]^{25}_D$ +8.3° (*c* 0.5, $CHCl_3$). ^{1}H NMR ($CDCl_3$, 500 MHz) δ 1.98, 2.01, 2.03, 2.04, 2.09, 2.10 (6s, 21H, 7 × OAc), 2.72−2.91 (m, 2H, Asn-β-CH_2), 3.65−3.78 (m, 3H, H-5′, H-5, H-4), 4.03 (dd, J = 2.5 Hz, 12.5 Hz, 1H, H-6″), 4.13 (m, 1H, H-6), 4.21 (t, J = 7.0 Hz, 1H, Fmoc-CH), 4.32−4.51 (m, 5H, Fmoc-CH_2, H-1′, H-6′, H-6‴), 4.57 (m, 1H, Asn-α-CH), 4.85 (t, J = 9.5 Hz, 1H, H-2), 4.92 (t, J = 9.5 Hz, 1H, H-2′), 5.07 (t, J = 9.5 Hz, 1H, H-4′), 5.14 (t, J = 9.5 Hz, 1H, H-3′), 5.21 (t, J = 9.5 Hz, 1H, H-1), 5.30 (t, J = 9.5 Hz, 1H, H-3), 6.19 (d, J = 8.5 Hz, 1H, Asn-α-NH), 6.68 (d, J = 9.0 Hz, 1H, 1-NH), 7.30 (app-t, 2H, Fmoc-Ar), 7.39 (app-t, 2H, Fmoc-Ar), 7.58 (d, J = 7.5 Hz, 2H, Fmoc-Ar), 7.75 (d, J = 7.5 Hz, 2H, Fmoc-Ar). ^{13}C NMR ($CDCl_3$, 125 MHz) δ 20.7, 20.8, 21.0, 37.8, 47.2, 50.5, 61.8 (C-6′), 61.9 (C-6), 67.8 (C-4′), 68.0, 71.0 (C-2′), 71.7 (C-5′), 72.1 (C-3′), 72.3 (C-2), 73.1 (C-3), 74.9 (C-5), 76.2 (C-4), 78.1 (C-1), 100.8 (C-1′), 120.2, 125.3, 127.3, 128.0, 141.4, 143.7, 143.8, 156.6, 169.3, 169.6, 170.0, 170.5, 170.8, 171.8, 171.9. FAB-HRMS calcd for $C_{45}H_{52}N_2O_{22}$: 972.3012. Found: 995.2883 [M + Na].

***N*$^\alpha$-(9-Fluorenylmethyloxycarbonyl)-*N*$^\omega$-[2,3,6-tri-*O*-acetyl-4-*O*-(2,3,4,6-tetra-*O*-acetyl-*β*-D-galactopyranosyl)-*β*-D-glucopyranosyl]-L-asparagine (6).** The *tert*-butyl ester of **6** was prepared from per-*O*-acetyl lactosyl azide[31] in 20% yield using method A and 28% using method B. $[\alpha]^{25}_D$ + 5.2° (*c* 0.4, $CHCl_3$). ^{1}H NMR ($CDCl_3$, 500 MHz) δ 1.44 (s, 9H, *t*-Bu), 1.97, 2.04, 2.06, 2.07, 2.08, 2.10, 2.15 (7s, 21H, 7 × OAc), 2.68−2.86 (m, 2H, Asn-β-CH_2), 3.71 (m, 1H, H-5), 3.77 (t, J = 9.5 Hz, 1H, H-4), 3.86 (m, 1H, H-5′), 4.06−4.16 (m, 3H, H-6, H-6″, H-6‴), 4.22 (t, J = 7.0 Hz, 1H, Fmoc-CH), 4.31 (t, J = 7.5 Hz, 1H, Fmoc-CH_2), 4.40−4.50 (m, 4H, Fmoc-CH_2, Asn-α-CH, H-1′, H-6′), 4.81 (t, J = 9.5 Hz, 1H, H-2), 4.95 (dd, J = 10.5 Hz, 3.5 Hz, 1H, H-3′), 5.12 (t, J = 10.5 Hz, 1H, H-2′), 5.21 (t, J = 9.0 Hz, 1H, H-1), 5.32 (t, J = 9.5 Hz, 1H, H-3), 5.36 (dd, J = 3.5 Hz, 1 Hz, 1H, H-4′), 5.95 (d, J = 8.5 Hz, 1H, Asn-α-NH), 6.38 (d, J = 9.0 Hz, 1H, 1-NH), 7.30 (app-t, 2H, Fmoc-Ar), 7.40 (app-t, 2H, Fmoc-Ar), 7.60 (d, J = 7.5 Hz, 2H, Fmoc-Ar), 7.75 (d, J = 7.5 Hz, 2H, Fmoc-Ar). ^{13}C NMR ($CDCl_3$, 100 MHz) δ 20.6, 20.7, 20.8, 20.9, 21.0, 28.0, 38.2, 47.2, 51.1, 60.0 (C-6′), 61.0(C-6), 66.7 (C-4′), 67.3, 69.1 (C-2′), 70.8 (C-2), 71.0 (C-3′), 71.1 (C-5′), 72.4 (C-3), 74.7 (C-5), 76.0 (C-4), 78.1 (C-1), 82.8, 101.0 (C-1′), 120.1, 125.3, 127.2, 127.8, 141.4, 143.9, 144.0, 156.3, 169.1, 169.5, 169.9, 170.2, 170.3, 170.4, 170.5, 170.7, 171.5. FAB-HRMS calcd for $C_{49}H_{60}N_2O_{22}Na$ [M + Na]$^+$: 1051.3518. Found: 1051.3515.

Compound **6** was obtained in quantitative yield from hydrolysis of the *tert*-butyl ester. $[\alpha]^{25}_D$ +15.7° (*c* 0.6, $CHCl_3$). ^{1}H NMR ($CDCl_3$, 500 MHz) δ 1.97, 2.05, 2.06, 2.06, 2.07, 2.10, 2.16 (7s, 21H, 7 × OAc), 2.73−2.91 (m, 2H, Asn-β-CH_2), 3.76−3.80 (m, 2H, H-5, H-4), 3.88 (m, 1H, H-5′), 4.04−4.18 (m, 3H, H-6, H-6″, H-6‴), 4.22 (t, J = 7.0 Hz, 1H, Fmoc-CH), 4.33−4.78 (m, 4H, Fmoc-CH_2, H-1′, H-6′), 4.58 (m, 1H, Asn-α-CH), 4.84 (t, J = 9.5 Hz, 1H, H-2), 4.95 (dd, J = 10.5 Hz, 3.5 Hz, 1H, H-3′), 5.10 (t, J = 10.5 Hz, 1H, H-2′), 5.23 (t, J = 9.0 Hz, 1H, H-1), 5.32 (t, J = 9.5 Hz, 1H, H-3), 5.36 (dd, J = 3.5 Hz, 1 Hz, 1H, H-4′), 6.20 (d, J = 8.5 Hz, 1H, Asn-α-NH), 6.68 (d, J = 9.0 Hz, 1H, 1-NH), 7.31 (app-t, 2H, Fmoc-Ar), 7.40 (app-t, 2H, Fmoc-Ar), 7.59 (d, J = 7.5 Hz, 2H, Fmoc-Ar), 7.76 (d, J = 7.5 Hz, 2H, Fmoc-Ar). ^{13}C NMR ($CDCl_3$, 125 MHz) δ 20.7, 20.9, 21.0, 21.1, 37.8, 47.2, 50.5, 60.9 (C-6′), 62.1 (C-6), 66.8 (C-4′), 67.7, 69.2 (C-2′), 70.8 (C-2), 71.1 (C-3′), 71.2 (C-5′), 72.6 (C-3), 74.9 (C-5), 76.1 (C-4), 78.1 (C-1), 101.1 (C-1′), 120.2, 125.3, 127.3, 128.0, 141.5, 143.8, 143.9, 156.6, 169.4, 169.9, 170.7, 170.8, 171.8, 172.7. FAB-HRMS calcd for $C_{45}H_{52}N_2O_{22}$: 972.3012. Found: 995.2924 [M + Na].

***N*$^\alpha$-(9-Fluorenylmethyloxycarbonyl)-*N*$^\omega$-[2,3,4-tri-*O*-acetyl-6-*O*-(2,3,4,6-tetra-*O*-acetyl-α-D-galactopyranosyl)-*β*-D-glucopyranosyl]-L-asparagine (7).** The *tert*-butyl ester of **7** was prepared from per-*O*-acetyl melibiosyl azide[31] in 10% yield using method A and 18% using method B. $[\alpha]^{25}_D$ +61.4° (*c* 0.4, $CHCl_3$). ^{1}H NMR ($CDCl_3$, 500 MHz) δ 1.44 (s, 9H, *t*-Bu), 1.96, 2.01, 2.05, 2.05, 2.06, 2.10, 2.16 (7s,

21H, 7 OAc), 2.68−2.90 (m, 2H, Asn-β-CH_2), 3.64−3.75 (m, 3H, H-5, H-6, H-6′), 4.03−4.06 (m, 2H, H-6″, H-6‴), 4.19 (t, J = 6.5 Hz, 1H, H-5′), 4.25 (t, J = 7.0 Hz, 1H, Fmoc-CH), 4.23−4.46 (m, 2H, Fmoc-CH_2), 4.52 (m, 1H, Asn-α-CH), 4.83 (t, J = 9.2 Hz, 1H, H-2), 5.02 (dd, J = 3.5 Hz, 11.0 Hz, 1H, H-2′), 5.08 (t, J = 9.2 Hz, 1H, H-4), 5.22 (t, J = 9.2 Hz, 1H, H-1), 5.27−5.35 (m, 3H, H-1′, H-3′, H-3), 5.42 (broad s, 1H, H-4′), 6.05 (d, J = 8.8 Hz, 1H, Asn-α-NH), 6.51 (d, J = 9.2 Hz, 1H, 1-NH), 7.31 (pseudo-t, 2H, Fmoc-Ar), 7.40 (pseudo-t, 2H, Fmoc-Ar), 7.62 (d, J = 7.2 Hz, 2H, Fmoc-Ar), 7.76 (d, J = 7.2 Hz, 2H, Fmoc-Ar). ^{13}C NMR ($CDCl_3$, 125 MHz) δ 20.7, 20.8, 20.9, 21.0, 21.1, 21.3, 28.1, 38.1, 47.3, 51.2, 61.9 (C-6′), 64.9 (C-6), 66.4 (C-5′), 67.4, 67.5 (C-3′), 68.1 (C-2′), 68.5 (C-4′), 68.7 (C-4), 70.7 (C-2), 72.9 (C-3), 74.7 (C-5), 77.9 (C-1), 82.4, 96.0 (C-1′), 120.0, 125.3, 127.1, 127.7, 141.2, 143.9, 156.2, 169.3, 169.8, 169.9, 170.1, 170.5, 170.8, 170.9, 171.2. FAB-HRMS calcd for $C_{49}H_{60}N_2O_{22}Na$ $[M + Na]^+$: 1051.3518. Found: 1051.3481.

Compound **7** was obtained in quantitative yield from hydrolysis of the *tert*-butyl ester. $[\alpha]^{25}_D$ +71.7° (*c* 0.6, $CHCl_3$). ^{1}H NMR ($CDCl_3$, 500 MHz) δ 1.98, 2.01, 2.04, 2.05, 2.08, 2.12, 2.15 (7s, 21H, 7 × OAc), 2.86 (m, 2H, Asn-β-CH_2), 3.51−3.66 (m, 2H, H-6, H-6′), 3.82 (m, 1H, H-5), 3.99−4.25 (m, 3H, Fmoc-CH, Fmoc-CH_2), 4.32 (m, 1H, H-5′), 4.41 (m, 2H, H-6″, H-6‴), 4.68 (m, 1H, Asn-α-CH), 4.85 (t, J = 9.2 Hz, 1H, H-2), 4.92 (t, J = 9.2 Hz, 1H, H-4), 5.07 (dd, J = 3.5 Hz, 11.0 Hz, 1H, H-2′), 5.20 (d, J = 3.5 Hz, 1H, H-1′), 5.25−5.32 (m, 3H, H-1, H-3′, H-3), 5.52 (broad s, 1H, H-4′), 6.05 (d, J = 8.8 Hz, 1H, Asn-α-NH), 6.51 (d, J = 9.2 Hz, 1H, 1-NH), 7.31 (app-t, 2H, Fmoc-Ar), 7.40 (app-t, 2H, Fmoc-Ar), 7.62 (d, J = 7.2 Hz, 2H, Fmoc-Ar), 7.76 (d, J = 7.2 Hz, 2H, Fmoc-Ar). ^{13}C NMR ($CDCl_3$, 125 MHz) δ 20.7, 20.80, 20.82, 21.0, 21.07, 21.13, 38.1, 47.2, 50.7, 62.3 (C-5′), 65.3 (C-6), 66.3 (C-6′), 67.7, 68.2 (C-3′), 68.3 (C-2′), 68.5 (C-4′), 69.2 (C-4), 70.8 (C-2), 72.9 (C-3), 74.7 (C-5), 78.0 (C-1), 95.6 (C-1′), 120.2, 125.3, 127.3, 128.0, 141.5, 143.88, 143.92, 156.4, 169.8, 170.2, 170.5, 170.8, 171.17, 171.24, 172.5. FAB-HRMS calcd for $C_{45}H_{52}N_2O_{22}$: 972.3012. Found: 995.2879 [M + Na].

Encoded Glycopeptide Library Synthesis. TentaGel S NH_2 resin (800 mg, 90-μm beads, 0.26 mmol/g loading) was used for the peptide library. TentaGel S NH_2 resin was first swelled in DMF overnight, then the beads were distributed equally into 17 reaction vessels (17 amino acids, except Cys, Met, Ile). The amino acid (3 equiv), HOBt (3 equiv), and DIC (3 equiv) were added to each reaction vessel. The amino acids were coupled for 2 h at room temperature with gentle shaking. A small sample of the resin solution from each reaction vessel was transferred into tiny test tubes to perform the Kaiser test. After all the couplings were completed, the resin was combined and transferred to a 10-mL polypropylene column with a frit at the bottom. The resin was washed with DMF (3 × 10 mL), methanol (3 × 10 mL), CH_2Cl_2 (3 × 10 mL), and DMF (3 × 10 mL). The N^{α}-Fmoc protecting group was removed by incubation twice in 6 mL of 20% piperidine/DMF for 15 min each. The resin was washed again with DMF (3 × 10 mL), methanol (3 × 10 mL), CH_2Cl_2 (3 × 10 mL), and DMF (3 × 10 mL). The cycle of resin distribution, amino acid coupling, Kaiser test, resin mixing, resin washing, Fmoc deprotection, and resin washing was repeated. The resin was swollen in 20 mL water for 24 h. Water was removed by suction, and the solution of AlocOSu (20.7 mg, 0.1 mmol) in CH_2Cl_2/diethyl ether (40 mL, 55/45 v/v) mixture and DIEA (94 μL, 0.54 mmol) were added to the wet beads. The mixture was shaken vigorously at room temperature for 30 min. The resin was washed three times with CH_2Cl_2/diethyl ether (55/45 v/v) and five times with DMF and dried by suction for 1 h. A few of the beads were transferred to a column and treated with 0.1% bromophenol blue in DMF at room temperature for 5 min. The beads were then washed with MeOH (5 × 1 mL) and water (5 × 1 mL) and transferred to a Petri dish, where they were observed under the microscope. The resin was distributed equally into seven reaction columns. The seven amino acid tags (3 equiv), HOBt (3 equiv), and DIC (3 equiv) were added to each reaction column. After each coupling, the resin was washed with DMF (3 × 10 mL), methanol (3 × 10 mL), CH_2Cl_2 (3 × 10 mL), and DMF (3 × 10 mL). $Pd(PPh_3)_4$ (4.2 mg, 0.25 equiv), $PhSiH_3$ (36 μL, 20 equiv) and CH_2Cl_2 (1 mL) were added to each reaction column to remove Aloc protecting groups. After 30 min, the resin was washed with CH_2Cl_2 (3 × 10 mL) and DMF (3 × 10 mL). The seven glycosylated amino acids (3 equiv), HBTU (3 equiv), HOBt (3 equiv), and DIEA (9 equiv) were added to each reaction column. After each coupling, the resin was pooled, mixed, washed, and Fmoc-deprotected. The cycle of resin distribution, amino acid coupling, Kaiser test, resin mixing, resin washing, Fmoc deprotection, and resin washing was repeated twice. After the amino acid assembly was completed, the carbohydrate acetyl protecting groups were removed by NaOMe (0.5 M, 0.5 mL) in methanol (5 mL) for 1 h, followed by washing with methanol (3 × 10 mL), CH_2Cl_2 (3 × 10 mL), and methanol (3 × 10 mL). The side-chain protection groups were removed using scavengers consisting of TFA 82.5%, EDT 2.5%, thioanisole 5%, phenol 5%, and H_2O 5% for 2.5 h. The resin was then washed with DMF (3 × 10 mL), methanol (3 × 10 mL), CH_2Cl_2 (3 × 10 mL), DMF (3 × 10 mL), 30% H_2O/DMF (3 × 10 mL), 60% H_2O/DMF (3 × 10 mL), H_2O (3 × 10 mL), and PBS buffer (3 × 10 mL) and stored in PBS at 4 °C.

Library Screening Against Lectins. The glycopeptide library was subjected to on-bead binding assays. A 200-μL portion of the bead-supported library (~250 000 beads) was transferred into a 1.5-mL polypropylene column with a polyethylene frit. The beads were washed with water (3 × 4 mL), PBS (3 × 4 mL), and PBS containing 0.05% Tween 20 (PBST) (3 × 4 mL), and then the resin was blocked with 1% BSA in PBS (PBSA) buffer solution (1 mL) for 1 h. The beads were filtered and washed with PBS (3 × 4 mL), PBST (3 × 4 mL), and PBSA (3 × 4 mL). The beads were then incubated with the fluorescent-labeled lectins (0.01 μg/mL) in PBSA (1 mL) for 1 h. The library was washed with PBST (3 × 4 mL), PBS (3 × 4 mL), and water (3 × 4 mL); transferred to a polystyrene Petri dish; and visualized using fluorescence microscopy. Bright beads were isolated with a pipet and treated with 6.0 M guanidine−HCl pH 1.0 solution to strip the protein off the beads. The positive beads were

then washed with double-distilled water three times. Each positive bead was transferred onto a micro TFA filter and submitted to protein sequencer for sequencing.

Parallel Synthesis of Lead Glycopeptides and Peptides 15−26 on Solid Support. TentaGel S NH_2 resin was used for the synthesis of lead glycopeptides and peptides. The TentaGel resin (200 mg, 0.26 mmol/g) was first partially coupled with Fmoc-Met-OH (0.2 equiv), HOBt (1.0 equiv), and DIC (1.0 equiv). After removing the Fmoc protecting group, the resin was distributed equally into 12 reaction columns. The six lead glycopeptides and peptides without GlcNAc were prepared by parallel methodology. The amino acids were coupled using HOBt and DIC, and the glycosylated amino acids were coupled using HBTU, HOBt, and DIEA. The Fmoc protecting group was removed using 20% piperidine in DMF. The carbohydrate acetyl protecting groups, and the amino acid side-chain protection groups were removed as described above.

Solid-Phase Binding Assays of Lead Glycopeptides and Peptides. Resin-bound lead glycopeptides and peptides were tested using a protocol similar to that for screening of the library. The assays were carried out in 1.0-mL polypropylene columns individually. The beads (20 μL) were blocked first with 1% BSA in PBS buffer solution (1 mL) for 1 h and then incubated with the fluorescent-labeled WGA lectin (0.05 μg/mL) in PBSA (1 mL) for 1 h. The resin was washed with PBST (3 × 4 mL), PBS (3 × 4 mL), and water (3 × 4 mL) and visualized using fluorescence microscopy.

Partial Cleavage of Lead Glycopeptides and Peptides. The lead glycopeptides and peptides on solid support were digested by CNBr. A small sample of the resin (about 20 beads) from each lead glycopeptide and peptide was transferred into a 200-μL micro centrifuge tube, and 100 μL of 0.1 M HCl was added, followed by addition 10 μL 2.0 M CNBr in CH_3CN. The resin was gently shaken overnight in the dark and lyophilized. The residue was analyzed by MALDI-MS.

Parallel Synthesis of Positive Glycopeptides 27−32. Rink amide MBHA resin was used for the synthesis of glycopeptides **27**−**32**. Reactions were run on a 25 μM scale using a 3-fold excess of amino acid. After synthesis, the resins were washed with DMF (3 × 4 mL), methanol (3 × 4 mL), and dichloromethane (3 × 4 mL) and dried. The peptides were cleaved from the resin and deprotected using 2 mL of cleavage solution (TFA/TIS/H_2O, 95:2.5:2.5) for 2 h. The solutions were concentrated and precipitated with diethyl ether. The precipitates were purified by RP-HPLC (100% H_2O). All peptides gave a single peak by HPLC and the expected mass by ion spray mass spectrometry.

NH_2−Ser-His-Asn(GlcNAc)-Gln-Gly−$CONH_2$ (27). A white powder was purified by HPLC in 47% yield. $[\alpha]^{26}_D$ −4.8° (*c* 0.5, H_2O). ^{1}H NMR (D_2O, 500 MHz) δ 2.07 (s, 3H, NAc), 2.08 (m, 1H), 2.21 (m, 1H), 2.44 (t, J = 7.5 Hz, 2H), 2.87 (m, 2H), 3.27 (m, 1H), 3.38 (m, 1H), 3.54 (m, 2H), 3.67 (t, J = 9.5 Hz, 1H), 3.79 (m, 1H), 3.87 (t, J = 10.0 Hz, 1H), 3.94 (m, 1H), 3.98 (m, 2H), 4.04 (m, 2H), 4.22 (t, J = 4.5 Hz, 1H), 4.39 (dd, J = 5.5 Hz, 8.5 Hz, 1H), 4.80 (m, 2H), 5.10 (d, J = 10.0 Hz, 1H, H-1), 7.38 (s, 1H), 8.70 (s, 1H). ^{13}C NMR (D_2O, 125 MHz) δ 22.3, 26.4, 26.8, 31.3, 36.6, 42.3, 50.4, 53.0, 53.7, 54.4, 54.6, 60.3, 60.8, 69.8, 74.4, 77.9, 78.6, 117.6, 128.3, 133.9, 168.1, 171.3, 172.4, 172.6, 173.7, 174.1, 175.0. FAB-HRMS calcd for $C_{28}H_{45}N_{11}O_{13}Na$ $[M + Na]^+$: 766.3091. Found: 766.3133.

NH_2−Phe-Arg-Asn(GlcNAc)-Ala-Ser−$CONH_2$ (28). A white powder was purified by HPLC in 52% yield. $[\alpha]^{26}_D$ −4.6° (*c* 0.3, H_2O). ^{1}H NMR (D_2O, 500 MHz) δ 1.46 (d, J = 6.5 Hz, 3H, CH_3), 1.59 (m, 2H, CH_2), 1.78 (m, 2H, CH_2), 2.05 (s, 3H, NAc), 2.88 (m, 2H), 3.25 (m, 4H), 3.50 (m, 2H), 3.65 (m, 1H), 3.76 (m, 1H), 3.87 (t, J = 11.0 Hz, 2H), 3.93 (m, 2H), 4.35 (m, 3H), 4.45 (m, 1H), 4.71 (m, 1H), 5.11 (d, J = 9.5 Hz, 1H, H-1), 7.33 (m, 2H), 7.44 (m, 3H). ^{13}C NMR (D_2O, 125 MHz) δ 16.7, 22.4, 24.5, 28.5, 36.7, 37.1, 40.7, 50.1, 50.3, 53.5, 54.5, 55.8, 60.7, 61.3, 69.7, 74.5, 77.8, 78.5, 128.2, 129.4, 129.6, 133.9, 156.9, 169.1, 172.3, 172.4, 172.5, 174.4, 175.0, 175.2. FAB-HRMS calcd for $C_{33}H_{54}N_{11}O_{12}$ $[M + H]^+$: 796.3984. Found: 796.3946.

NH_2−Arg-His-Asn(GlcNAc)-Phe-Ala−$CONH_2$ (29). A white powder was purified by HPLC in 62% yield. $[\alpha]^{26}_D$ +4.3° (*c* 0.4, H_2O). ^{1}H NMR (D_2O, 500 MHz) δ 1.40 (d, J = 6.5 Hz, 3H, CH_3), 1.66 (m, 2H, CH_2), 1.95 (m, 2H, CH_2), 2.05 (s, 3H, NAc), 2.79 (m, 2H), 3.07 (m, 1H), 3.13 (d, J = 6.5 Hz, 2H), 3.24 (m, 3H), 3.51 (m, 2H), 3.65 (t, J = 7.5 Hz, 1H), 3.77 (m, 1H), 3.84 (t, J = 10.0 Hz, 1H), 3.91 (m, 1H), 4.08 (m, 1H), 4.30 (m, 1H), 4.64 (m, 1H), 4.70 (d, J = 7.0 Hz, 2H), 5.06 (d, J = 9.5 Hz, 1H, H-1), 7.09 (s, 1H), 7.33 (m, 3H), 7.39 (m, 3H), 8.64 (s, 1H). ^{13}C NMR (D_2O, 125 MHz) δ 16.9, 22.3, 23.7, 26.6, 28.3, 36.6, 37.1, 40.6, 49.7, 50.0, 52.7, 54.5, 55.3, 60.7, 69.7, 74.3, 77.8, 78.6, 115.4, 117.4, 117.7, 127.5, 128.0, 129.0, 129.5, 133.9, 136.5, 157.0, 169.6, 170.9, 171.9, 172.4, 172.7, 175.0, 177.5. FAB-HRMS calcd for $C_{36}H_{56}N_{13}O_{11}$ $[M + H]^+$: 846.4217. Found: 846.4221.

NH_2−Arg-Gln-Asn(GlcNAc)-Gly-Asn−$CONH_2$ (30). A white powder was purified by HPLC in 42% yield. $[\alpha]^{26}_D$ +7.4° (*c* 0.3, H_2O). ^{1}H NMR (D_2O, 500 MHz) δ 1.72 (m, 2H, CH_2), 1.99 (m, 2H, CH_2), 2.06 (s, 3H, NAc), 2.11 (m, 2H, CH_2), 2.43 (m, 2H, CH_2), 2.80 (m, 2H, CH_2), 2.88 (m, 2H, CH_2), 3.28 (m, 2H), 3.53 (m, 2H), 3.67 (t, J = 9.0 Hz, 1H), 3.78 (m, 1H), 3.87 (t, J = 10.0 Hz, 1H), 3.93 (m, 1H), 4.01 (m, 2H), 4.12 (m, 1H), 4.43 (m, 1H), 4.79 (m, 2H), 5.10 (d, J = 9.5 Hz, 1H, H-1). ^{13}C NMR (D_2O, 125 MHz) δ 22.4, 23.7, 27.0, 28.3, 31.1, 36.6, 36.9, 40.7, 42.9, 50.4, 50.5, 52.9, 53.6, 54.5, 60.9, 69.8, 74.5, 77.9, 78.6, 113.2, 115.5, 117.8, 157.0, 163.1, 163.4, 169.8, 171.3, 172.6, 172.8, 172.9, 174.8, 175.0, 175.3, 177.9. FAB-HRMS calcd for $C_{29}H_{52}N_{13}O_{13}$ $[M + H]^+$: 790.3802. Found: 790.3843.

NH_2−Val-His-Asn(GlcNAc)-Arg-Gln−$CONH_2$ (31). A white powder was purified by HPLC in 45% yield. $[\alpha]^{26}_D$ −2.5° (*c* 0.4, H_2O). ^{1}H NMR (D_2O, 500 MHz) δ 1.03 (m, 6H, $2CH_3$), 1.68 (m, 2H, CH_2), 1.88 (m, 2H, CH_2), 2.04 (s, 3H, NAc), 2.07 (m, 1H), 2.21 (m, 2H, CH_2), 2.42 (m, 2H, CH_2), 2.85 (m, 2H, CH_2), 3.26 (m, 4H), 3.51 (m, 2H), 3.65 (t, J = 9.0 Hz, 1H), 3.78 (m, 1H), 3.84 (t, J = 10.0 Hz, 1H), 3.88 (m, 2H), 4.33 (m, 2H), 4.74 (m, 2H), 5.07 (d, J = 9.5 Hz, 1H, H-1), 7.36 (s, 1H), 8.68 (s, 1H). ^{13}C NMR (D_2O, 125 MHz) δ 22.3, 24.7, 26.4, 27.0, 28.1, 30.2, 31.6, 36.7, 40.7, 50.3, 52.9, 53.3, 54.0, 54.5, 58.5, 60.7, 69.7, 74.4, 77.8, 78.6, 115.4, 117.5, 117.7, 128.3, 134.0, 157.0, 169.6, 171.2,

172.4, 172.5, 173.8, 175.0, 176.0, 178.1. FAB-HRMS calcd for $C_{34}H_{59}N_{14}O_{12}$ $[M + H]^+$ 855.4431. Found: 855.4400.

NH_2−Phe-Val-Asn(GlcNAc)-Ser-Arg−$CONH_2$ (32). A white powder was purified by HPLC in 66% yield. $[\alpha]^{26}_D$ −9.1° (*c* 0.4, H_2O). ^1H NMR (D_2O, 500 MHz) δ 0.93 (m, 6H, $2CH_3$), 1.69 (m, 2H, CH_2), 1.88 (m, 2H, CH_2), 2.03 (s, 3H, NAc), 2.88 (m, 2H, CH_2), 3.25 (m, 6H), 3.49 (m, 2H), 3.64 (t, $J = 9.0$ Hz, 1H), 3.76 (m, 1H), 3.86 (m, 5H), 4.11 (m, 1H), 4.36 (m, 3H), 4.44 (m, 1H), 4.76 (m, 2H), 5.10 (d, $J = 9.5$ Hz, 1H, H-1), 7.30 (m, 2H), 7.41 (m, 3H). ^{13}C NMR (D_2O, 125 MHz) δ 18.1, 18.4, 22.5, 24.7, 28.2, 28.4, 30.6, 30.7, 36.7, 37.2, 40.8, 50.0, 53.4, 53.4, 54.4, 54.6, 56.1, 59.5, 59.7, 60.8, 61.2, 61.3, 69.8, 74.5, 77.9, 78.6, 128.2, 129.4, 129.7, 134.0, 157.0, 169.2, 172.0, 172.3, 172.6, 175.0, 176.4. FAB-HRMS calcd for $C_{35}H_{58}N_{11}O_{12}$ $[M + H]^+$: 824.4261. Found: 824.4268.

Modeling. Molecular dynamics calculations were carried out on a SGI workstation using the MacroModel 7.0 program. The coordinates from the crystal structure of WGA3 complexed with GlcNAcβ1,6Gal (PDB code: 1K7T) were used as input for calculations after removal of GlcNAcβ1,6Gal and water.[25] To compare their binding interactions with the receptor, the protein was fixed, and peptides were initially energy-minimized and superimposed with the GlcNAc position. The calculation was carried out by the simulated annealing method. The starting temperature was 350 K, decreasing to 298 K in 0.5-fs steps, with 5000 subsequent cycles of conjugate gradient positional refinement.

Fluorescence Measurements of Glycopeptides Binding to WGA. A WGA stock solution was made in 2 mg/mL in PBS buffer and diluted to a final concentration of 4.3 μM in PBS buffer (pH 7.2). The glycopeptide stock solutions were prepared in ∼10 to 15 mg/mL in PBS buffer (pH 7.2). Fluorescence measurements were performed with the Cary-Eclipse spectrofluorimeter. All measurements were performed in 1-cm quartz cuvettes at room temperature with excitation at 280 nm. Solutions of WGA and glycopeptide were prepared by mixing 80 μL of WGA solution (2 mg/mL), 10−300 μL of glycopeptide solution (∼10 to 15 mg/mL), and PBS buffer to bring the volume to 1.5 mL. The fluorescence intensities of each solution relative to that of a reference solution containing only WGA and buffer were immediately determined. The absorption at 280 nm and the fluorescence at the appropriate wavelengths of solutions of the glycopeptide alone in buffer were also measured and were used to correct the observed fluorescence of the WGA/glycopeptide solutions. The relative fluorescence intensity of WGA saturated with glycopeptide, F_∞, was obtained by extrapolating a plot of $1/(F_0 - F)$ versus 1/[C] at $1/[C] = 0$, where F was the measured fluorescence of a solution of WGA complexed with a given glycopeptide concentration [C], and F_0 was the fluorescence of a solution WGA alone. The association constants were determined by plotting log $[(F_0 - F)/(F - F_\infty)]$ against log[C], where F_0, F, and F_∞ were the fluorescence intensities of solution of WGA alone, WGA in the presence of a concentration [C] of glycopeptide, and WGA saturated with glycopeptide, respectively. The value of $-\log K_a$ for the complex equals the value of log[C] at $\log[(F_0 - F)/(F - F_\infty)] = 0$.

Acknowledgment. This paper was taken in part from the dissertation of Laiqiang Ying, University of California, Davis, 2004. This work was supported by National Science Foundation CHE-0196482. NSF CRIF program (CHE-9808183), NSF Grant OSTI 97-24412, and NIH Grant RR11973 provided funding for the NMR spectrometers used on this project.

References and Notes

(1) *Essentials of Glycobiology*; Varki, A., Cummings, R., Esko, J., Freeze, H., Hart, G., Marth, J., Eds.; Cold Spring Harbor Laboratory Press: Cold Spring Harbor, NY, 1999; pp 455−467.

(2) (a) Ramstroem, O.; Lohmann, S.; Bunyapaiboonsri, T.; Lehn, J.-M. *Chem.−Eur. J.* **2004**, *10*, 1711−1715. (b) Baytas, S. N.; Linhardt, R. J. *Mini-Rev. Org. Chem.* **2004**, *1*, 27−39. (c) Amaya, T.; Tanaka, H.; Takahashi, T. *Synlett* **2004**, *3*, 497−502. (d) Kanemitsu, T.; Kanie, O. *Comb. Chem. High Throughput Screening* **2002**, 5, 339−360. (e) Marcaurelle, L. A.; Seeberger, P. H. *Curr. Opin. Chem. Biol.* **2002**, *6*, 289−296. (f) Kanie, O.; Hindsgaul, O. *Solid Support Oligosaccharide Synthesis and Combinatorial Carbohydrate Libraries*; 2001, pp 239−256. (g) Seeberger, P. H.; Haase, W.-C. *Chem. Rev.* **2000**, *100*, 4349−4393. (h) Ye, X.-S.; Wong, C.-H. *J. Org. Chem.* **2000**, *65*, 2410−2431. (i) Zhang, Z.; Ollmann, I. R.; Ye, X.-S.; Wischnat, R.; Baasov, T.; Wong. C.-H. *J. Am. Chem. Soc.* **1999**, *121*, 734−753. (j) Zhu, T.; Boons, G.-J. *Angew. Chem., Int. Ed.* **1998**, *37*, 1898−1900.

(3) Christensen, M. K.; Meldal, M.; Bock, K.; Cordes, H.; Mouritsen, S.; Elsner, H. *J. Chem. Soc., Perkin Trans. 1* **1994**, 1299−1310.

(4) Lin, C.-C.; Shimazaki, M.; Heck, M.-P.; Wang, R.; Kimura, T.; Ritzen, H.; Takayama, S.; Wu, S.-H.; Weitz-Schmidt, G.; Wong, C.-H. *J. Am. Chem. Soc.* **1996**, *118*, 6826−6840.

(5) Schleyer, A.; Meldal, M.; Manat, R.; Paulsen, H.; Bock, K. *Angew. Chem., Int. Ed.* **1997**, *36*, 1976−78. Halkes, K. M.; Gotfredsen, C. H.; Grotli, M.; Miranda, L. P.; Duus, J. O.; Meldal, M. *Chemistry* **2001**, *7*, 3584−3589.

(6) Mathieux, N.; Paulsen, H.; Meldal, M.; Bock, K. *J. Chem. Soc., Perkin Trans. 1* **1997**, 2359−2368.

(7) Lam, K. S.; Salmon, S. E.; Hersh, E. M.; Hruby, V. J.; Kazmierski, W. M.; Knapp, R. J. *Nature (London)* **1991**, *354*, 82−84. Furka, A.; Sebestyan, F.; Asgedom, M.; Dibo, G. *Int. J. Pept. Res.* **1991**, *37*, 487−493.

(8) St. Hilaire, P. M.; Lowary, T. L.; Meldal, M.; Bock, K. *J. Am. Chem. Soc.* **1998**, *120*, 13312−13320.

(9) Halkes, K. M.; St. Hilaire, P. M.; Crocker, P. R.; Meldal, M. *J. Comb. Chem.* **2003**, *5*, 18−27.

(10) Youngquist, R. S.; Fuentes, G. R.; Lacey, M. P.; Keough, T. *J. Am. Chem. Soc.* **1995**, *117*, 3900−3906.

(11) Lebl, M.; Lam, K. S.; Salmon, S. E.; Krchnak, V.; Sepetov, N.; Kocis, P. U.S. Patent 5840485, 1998.

(12) Vagner, J.; Barany, G.; Lam, K. S.; Krchnak, V.; Sepetov, N. F.; Ostrem, J. A.; Strop, P.; Lebl, M. *Proc. Natl. Acad. Sci. U.S.A.* **1996**, *93*, 8194−8199.

(13) Debenham, S. D.; Snyder, P. W.; Toone, E. J. *J. Org. Chem.* **2003**, *68*, 5805−5811.

(14) Liu, R.; Marik, J.; Lam, K. S. *J. Am. Chem. Soc.* **2002**, *124*, 7678−7680.

(15) Kaiser, E.; Colescott, R. L.; Bossinger, C. D.; Cook, P. I. *Anal. Biochem.* **1970**, *34*, 595−598.

(16) Grieco, P.; Gitu, P. M.; Hruby, V. J. *J. Pept. Res.* **2001**, *57*, 250−256.

(17) Sjolin, P.; Elofsson, M.; Kihlberg, J. *J. Org. Chem.* **1996**, *61*, 560−565.

(18) Reagent K: phenol/thioanisole/H_2O/EDT/TFA (0.75:0.5:0.5:0.25:10, w/v/v/v/v).
(19) Nagata, Y.; Burger, M. M. *J. Biol. Chem.* **1974**, *249*, 3116−3122.
(20) Lotan, R.; Sharon, N. *Biochem. Biophys. Res. Commun*. **1973**, *55*, 1340−1346.
(21) Privat, J. P.; Delmotte, F.; Mialonier, G.; Bouchard, P.; Monsigny, M. *Eur. J. Biochem*. **1974**, *47*, 5−14.
(22) Jordan, F.; Bassett, E.; Redwood, W. R. *Biochem. Biophys. Res. Commun*. **1977**, *75*, 1015−1021.
(23) Wright, C. S. *J. Mol. Bio*. **1984**, *178*, 91−104.
(24) Bains, G.; Lee, R. T.; Lee, Y. C.; Freire, E. *Biochemistry* **1992**, *31*, 12624−12628.
(25) Muraki, M.; Ishimura, M.; Harata, K. *Biochim. Biophys. Acta* **2002**, *1569*, 10−20.
(26) Wittmann, V.; Seeberger, S. *Angew. Chem., Int. Ed.* **2004**, *43*, 900−903.
(27) Antonenko, V. V.; Mortezaei, R.; Kulikov, N. V. *Methods Princ. Med. Chem.* **2000**, *7*, 39−80.
(28) Scott, J. K.; Smith, G. P. *Science* **1990**, *249*, 386−390.
(29) Chipman, D. M.; Grisaro, V.; Sharon, N. *J. Biol. Chem.* **1967**, *242*, 4388−4394.
(30) Allen, A. K.; Neuberger, A.; Sharon, N. *Biochem. J.* **1973**, *131*, 155−162.
(31) Petö, C.; Batta, G.; Györgydeák, Z.; Sztaricskai, F. *Liebigs Ann. Chem.* **1991**, 505−507.
(32) Inazu, T.; Kobayashi, K. *Synlett* **1993**, 869−870.

CC049836E